Laser Photonics Rev. **5**, No. 6, 737–749 (2011) / **DOI** 10.1002/lpor.201000036

LASER & PHOTONICS REVIEWS

Abstract Over the last fifteen years, a series of theoretical and experimental investigations have demonstrated the usefulness of circular geometries to tailor second-order nonlinear optical effects. However, until recently, such effects have remained rather weak, calling for their enhancement. In parallel, developments in the field of high quality factor spherical or ring resonators have shown that many different types of light-matter interactions can be dramatically amplified when light is coupled in the whispering gallery modes of such resonators. In high-quality spherical micro-resonators, close to one million interactions can occur between a nonlinear molecule and a circulating light pulse. Recent research on nonlinear optics in spherical geometry is reviewed, from micrometer-size spheres to whispering gallery mode resonators.

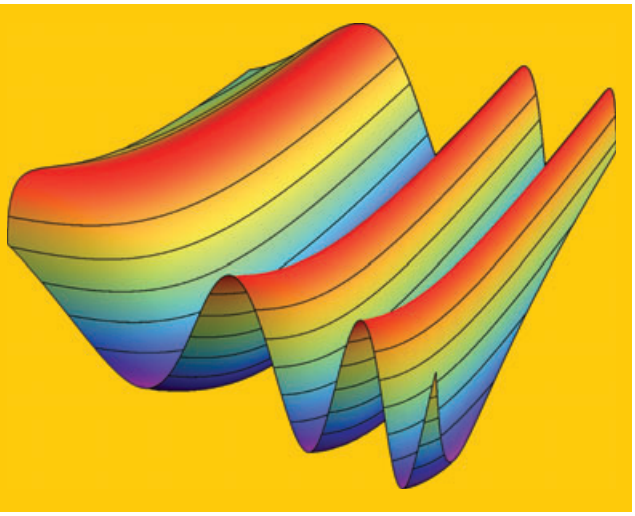

Nonlinear optics in spheres: from second harmonic scattering to quasi-phase matched generation in whispering gallery modes

Gregory Kozyreff[1,*], Jorge Luis Dominguez-Juarez[2], and Jordi Martorell[2,3,*]

1. Introduction

In nonlinear optics, quadratic effects require the inversion symmetry to be broken. This can happen either in the bulk of crystals lacking that symmetry or at the interface between two media. In the latter configuration, any molecule, fluorescent or non-fluorescent, can in principle exhibit a second-order nonlinear response to an optical signal. Such a response, however, is usually extremely weak and requires one to match the phase velocities of the interacting waves. Traditionally, birefringent non-centrosymmetric inorganic crystals have been used to efficiently up- or down-convert the frequency of an incoming laser beam. To match the phase velocities, an alternative route to birefringence is to introduce a periodic modulation of the index of refraction in the same direction as the beam propagation leading to what is known as quasi-phase matching [1]. Birefringence and quasi-phase matching have been effectively used to obtain laser light at almost any frequency within the ultraviolet (UV), visible, and infrared ranges. There are, however, many other applications that would benefit from a mechanism capable of generating light from a non-fluorescent source, but cannot afford to be implemented in dense matter, birefringent, or non-centrosymmetric configurations. Over the last fifteen years, a large body of research conducted involving circular geometries has completely renewed the perspective on tailoring second-order nonlinear light generation.

1.1. Second harmonic scattering from small spheres

In 1995, it was proposed and experimentally demonstrated that the use of dielectric spheres with diameters close to one wavelength of the generated wave and coated with a nonlinear material could obviate the need to use non-centrosymmetric materials at a macroscopic scale [2, 3]. The electric field vector at the entrance side of the sphere would interact with molecules that point at a given direction. At the exit of the sphere, both field and molecules would have changed orientation, making the second harmonic (SH) signal on both sides add constructively. Such a, to a certain extent, naive picture of the nonlinear interaction on a sphere surface was confirmed by the results of a model that considered SH scattering in the Rayleigh-Gans-Debye approximation (see below) from single spheres whose diameter was close to the wavelength of light [4]. Second harmonic generation (SHG) was configured in two large lobes on the scattering plane symmetrically located relative to the forward direction. Such characteristic features of the SH

[1] Optique Nonlinéaire Théorique, Université Libre de Bruxelles (ULB), CP 231, Campus de la Plaine, 1050 Bruxelles, Belgium
[2] ICFO-Institut de Ciencies Fotoniques, Mediterranean Technology Park, 08860 Castelldefels (Barcelona), Spain
[3] Departament de Física i Enginyeria Nuclear, Universitat Politècnica de Catalunya, Terassa, Spain
[*] Corresponding authors: e-mail: gkozyref@ulb.ac.be, jordi.martorell@icfo.es

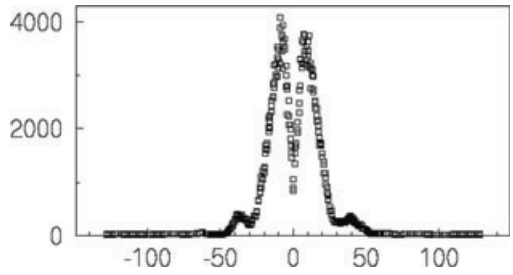

Figure 1 Experimental SH scattering intensity (counts/10s) as a function of scattering angle (in degrees) for a suspension of polystyrene spheres with adsorbed malachite green on their surfaces. (Reprinted with permission from [7]. ©2001 American Physical Society.)

scattering from small spheres could not be made apparent in the first experimental observation because it considered an ordered three-dimensional array of many spheres, otherwise known as a colloidal or photonic crystal [2–5]. Surprisingly, although generation from disordered distributions of spheres was already considered late in 1996 [6], it was not until 2001 when vanishing SH scattering in the direction of the incoming field, together with the lobe structure predicted by the modified Rayleigh-Gans-Debye model, were observed experimentally [7]. The experimentally recorded radiation diagram is shown Fig. 1.

Parallel to the experimental work, an increasing interest developed in the theoretical study of the second-order nonlinear interaction in circular geometries. Early work on the subject was limited to the study of small spheres, i.e. limited to $ka \ll 1$, where k and a are the fundamental wave number and sphere radius, respectively. In this Rayleigh limit, the dipole and quadrupole radiations are of the same strength for the SH, and the SH intensity was predicted to scale as $(ka)^6$ [8–10]. This suggested that a very effective conversion could be obtained if large spheres were to be considered. Unfortunately, calculations for arbitrary sizes (Mie scattering) reported in 2004 indicated that when the size parameter $ka \approx 1$, the scattering efficiency begins to deviate from the Rayleigh-based theory [11]. Past this value, the scattering efficiency grows slowly with the size parameter and exhibits several resonances somehow similar to those found in the linear Mie scattering theory. Theoretical studies of two-dimensional circular geometries that considered a Mie-type solution arrived at similar conclusions [12, 13]. A simpler approach than the full Mie scattering theory, the nonlinear Rayleigh-Gans-Debye theory assumes that the index contrast between the sphere and the surrounding medium is sufficiently small such that the fundamental field inside the sphere is an unperturbed plane wave [4, 7]. This yields manageable expressions for the SH power for spheres with $ka \approx 1$, which are consistent with the Rayleigh theory of [8] when $ka \ll 1$ and agree well with experiments [7]. The approach was recently applied to finite cylindrical particles [14]. The nonlinear Wentzel-Kramers-Brillouin theory is the first-order correction of the Rayleigh-Gans-Debye theory in the index contrast. It still assumes that the fundamental field inside the sphere is a plane wave of constant amplitude, but undergoes a phase shift as it goes through the second half of the sphere [15]. Recently, a systematic experimental investigation of SH scattering as a function of size parameter was conducted with polystyrene spheres [16]. The trend observed experimentally agreed well with the predictions of the nonlinear Mie scattering theory and, also, with the nonlinear Wentzel-Kramers-Brillouin model. On the contrary, the Rayleigh-Gans-Debye theory was found to be strongly inaccurate for ka larger than 1. The study also showed that, for a given solid angle detection window, generation was maximized when the size parameter was between 3 and 5; beyond 5, it gradually decreased with some more or less pronounced oscillations.

1.2. Photonic crystal strategy to enhance scattered SHG

To enhance the signal from a single sphere, one of the strategies is to add coherently the SH light scattered from more than one sphere. In this respect, it is a fortunate fact that large concentrations of nanometer-size polystyrene spheres in water self-organize in an fcc crystalline lattice forming a colloidal or photonic crystal. From such an ordered structure, it is possible to take advantage of the refractive index dispersion at the edges of the photonic band gap. Indeed, if the SH frequency is tuned close to the low-frequency edge of the band, the effective index decreases. On the other hand, the fundamental frequency usually lies far from any photonic band and, therefore, propagates as if traversing a homogeneous medium (an exception to this rule is found in Ref. [17]). In 1970, Bloembergen and Sievers proposed this effect as a way to achieve phase matching, and indeed a peak of SHG could be clearly identified when measured from an ordered distribution of coated spheres [5]. Such a structural phase matching mechanism was also used for SHG using opals made of silicon spheres [17] or to enhance third harmonic generation from opals of polystyrene spheres [18].

To increase the surface nonlinearity, crystal violet (CV) molecules were chemically bound to carboxylic groups on sphere surfaces [19]. The negatively charged surface sulfate groups were not screened by the positively charged nonlinear molecules and very good quality nonlinear colloidal crystals could be formed. CV exhibits a relatively large nonlinearity when deposited on a glass substrate. Each CV molecule contains three aromatic rings that, when the molecule is at an interface, bend to form a tetrahedron [20] that occupies a volume of approximately $0.02\,\mathrm{nm}^3$. This tetrahedron could be linked to the second-order nonlinear response of the molecule. A weak, but visible to the naked eye, SH beam was generated from a 200 µm thick macroscopically centrosymmetric material [21]. Yet, molecular absorption, sphere size dispersion, and structural defects in the crystalline lattice proved to be limiting factors to reach quadratic growth of the SHG versus the colloidal crystal path length [22]. To achieve the goal of light generation from a small number of non-fluorescent molecules, an alternative configuration that would take advantage of the symmetry

breaking at the surface but that would not be limited by strong absorption or scattering was needed.

1.3. SHG in whispering gallery modes

Parallel to the study of the nonlinear interaction in small spheres, there has been an increasing interest in enhancing such nonlinear interaction by taking advantage of the high quality factors of spherical micro-resonators when light is coupled into the whispering gallery modes (WGMs). Pioneering work in the field considered, first, discs instead of spheres [23–25]. In such a geometry, a quasi-phase matching mechanism could be implemented by periodically poling a lithium niobate slab, which was polished down to a 3 mm diameter disc [26]. An alternative to quasi-phase matching is a modal phase matching that was implemented in a silica toroidal ring micro-resonator for third harmonic generation [27]. These configurations are interesting in terms of the fabrication of micrometer-size solid-state devices for light generation, but they would present similar handicaps as the photonic crystal mentioned above if one were to consider them for the detection of molecules that could be highly absorptive at the wavelength of interest. Coating microsphere surfaces with nonlinear molecules is a more versatile alternative [28, 29]. In such a configuration, only the evanescent tail of the electromagnetic field coupled into a WGM would interact with the nonlinear absorptive molecule. The rest of the field would travel within a highly transparent medium, such as fused quartz. Such a configuration poses many challenges, an important one being the ability to implement a phase matching or quasi-phase matching mechanism in order that the contribution from each round trip of the light beam would add coherently with the contribution from the previous one. As opposed to a small sphere, where phase matching within the sphere plays a little or no role at all [16], a high-Q cavity-enhanced interaction demands a phase matching or quasi-phase matching mechanism. Further challenges arise if a pulsed operation is considered, such as a group velocity dispersion that would quickly lead to a walk-off between the fundamental and SH waves. Another important question associated with micro-resonators is how to efficiently couple light into them. Most often, an eroded or tapered fiber is used, which must be carefully designed and positioned to inject a maximum amount of light into the micro-cavity [30–38]. For a recent and general review on the physics and applications of WGM resonators, we refer readers to the authoritative papers by Matsko and Ilchenko [39, 40].

This review continues with two sections that discuss the theory and experimental issues related to second-order effects with WGMs. Section 2 presents a heuristic approach to account for the nonlinear interaction when the fields are coupled in WGMs. The various options for phase matching are discussed and predictions useful for implementing an adequate configuration to obtain an effective quasi-phase matching are proposed. In Sect. 3, we discuss practical experimental issues related to the generation and observation of SH waves with WGMs, eventually leading to a detectable change in SHG by less than 100 molecules attached to the surface of a microsphere. Finally in Sect. 4, we discuss some opportunities of applications afforded by the latest advances in second-order effects with WGMs.

2. Theory for SHG with WGMs

As depicted schematically in Fig. 2, light in a WGM is concentrated near the equator of a spherical cavity. A fully vectorial theory of the nonlinear interaction of WGMs based on Maxwell's equations is given in [28]. In this section, we provide a shorter, plausible theoretical treatment by performing slight readjustments of the usual textbook theory of nonlinear wave mixing. A similar approach is followed in [41] to describe SHG in micro-ring AlGaAs resonators.

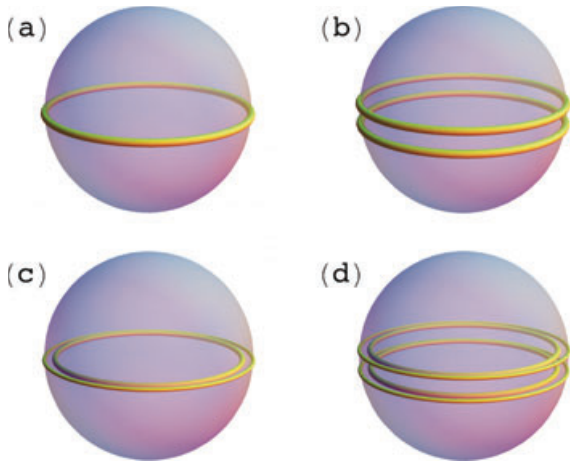

Figure 2 (online color at: www.lpr-journal.org) Sketch of WGM intensity distribution within a sphere. WGMs are characterized by orbital numbers $l \gg 1$ and $l - |m| = O(1)$, $p = O(1)$, where m and p are the azimuthal and radial numbers, respectively. The number of intensity maxima in the radial direction is given by p; likewise, $l - |m| + 1$ is the number of intensity maxima in the polar direction near the equator. (a) Radial number $p = 1$, $m = l$; (b) $p = 1$, $m = l - 1$; (c) $p = 2$, $m = l$; (d) $p = 2$, $m = l - 1$.

In view of Fig. 2a, let us first assume that the electric field can locally be written as

$$E = \alpha_1(s,t)\mathrm{e}^{\mathrm{i}k_1 s - \mathrm{i}\omega_1 t} + \alpha_2(s,t)\mathrm{e}^{\mathrm{i}k_2 s - \mathrm{i}\omega_2 t} + \text{c.c.}, \quad (1)$$

where α_i are slowly varying amplitudes and s is a tangent coordinate. With this ansatz, and for a suitable normalization of α_i, one easily arrives at the coupled wave equations [42]

$$\left(\frac{\partial}{\partial t} + v_1\frac{\partial}{\partial s} + \Gamma_1\right)\alpha_1 = \mathrm{i}\chi^{(2)}\alpha_2\alpha_1^*\mathrm{e}^{-\mathrm{i}\Delta k s + \mathrm{i}\Delta\omega t} \quad (2)$$

$$\left(\frac{\partial}{\partial t} + v_2\frac{\partial}{\partial s} + \Gamma_2\right)\alpha_2 = \mathrm{i}\chi^{(2)}\alpha_1^2\mathrm{e}^{\mathrm{i}\Delta k s - \mathrm{i}\Delta\omega t}, \quad (3)$$

where v_i are group velocities, Γ_i are loss coefficients, and $\chi^{(2)}$ is the appropriate component of the nonlinear susceptibility tensor. Furthermore,

$$\Delta k = 2k_1 - k_2, \qquad \Delta\omega = 2\omega_1 - \omega_2. \quad (4)$$

Hence, phase matching is locally achieved by making $\Delta k = 0$, which, for plane waves, means conservation of linear momentum.

Next, let us express the fact that waves follow closed trajectories along a sphere of radius a and that the frequencies ω_i are resonant. We do this by imposing the periodic boundary conditions

$$\alpha_i(2\pi a, t) = \alpha_i(0, t)\,. \tag{5}$$

Integrating (2) and (3) with respect to s over the sphere circumference then yields

$$\frac{\partial \alpha_1}{\partial t} + \Gamma_1 \alpha_1 = \frac{\mathrm{i}}{2\pi a}\int_0^{2\pi a} \chi^{(2)} \alpha_2 \alpha_1^* \mathrm{e}^{-\mathrm{i}\Delta k s + \mathrm{i}\Delta\omega t}\mathrm{d}s \tag{6}$$

$$\frac{\partial \alpha_2}{\partial t} + \Gamma_2 \alpha_2 = \frac{\mathrm{i}}{2\pi a}\int_0^{2\pi a} \chi^{(2)} \alpha_1^2 \mathrm{e}^{\mathrm{i}\Delta k s - \mathrm{i}\Delta\omega t}\mathrm{d}s\,. \tag{7}$$

Finally, if the nonlinear interaction is sufficiently weak, the amplitudes α_i vary only little over the distance $2\pi a$. Hence, to first order in $\chi^{(2)}$, we may neglect spatial variation of α_i in the integrals above and, eventually, we obtain

$$\frac{\mathrm{d}\alpha_1}{\mathrm{d}t} + \Gamma_1 \alpha_1 = \mathrm{i}\kappa^* \alpha_2 \alpha_1^* \mathrm{e}^{\mathrm{i}\Delta\omega t} \tag{8}$$

$$\frac{\mathrm{d}\alpha_2}{\mathrm{d}t} + \Gamma_2 \alpha_2 = \mathrm{i}\kappa \alpha_1^2 \mathrm{e}^{-\mathrm{i}\Delta\omega t}\,, \tag{9}$$

where

$$\kappa = \frac{1}{2\pi a}\int_0^{2\pi a} \chi^{(2)} \mathrm{e}^{\mathrm{i}\Delta k s}\mathrm{d}s \tag{10}$$

is the coupling constant between the fundamental and SH modes.

Equations (8) and (9) form a typical model for nonlinear wave mixing in microspheres and other circular resonators [23, 43–46], which can easily be generalized to larger sets of modes. Four-wave mixing mediated by $\chi^{(3)}$ can obviously be treated along the same lines. From the above discussion, the natural description of SHG in spheres is in terms of coupled modes, rather than free-propagating waves. To obtain an efficient energy conversion between the modes, the resonance condition $\Delta\omega \ll \Gamma_1, \Gamma_2$ should be met. On the other hand, phase matching now arises through an integral expression of the type given in (10) for the nonlinear coupling constant κ between modes. A lack of phase matching would result in a vanishing κ. Finally, if $\Delta k \neq 0$, Eq. (10) also suggests ways to engineer a space-varying $\chi^{(2)}$ to obtain a non-zero κ.

However, the above expression for the coupling constant is clearly overly simplified. Indeed the plane waves ansatz $\exp(\mathrm{i}k_i s)$ in (1) can at most be a locally valid representation of the modes circulating in the sphere. In the course of propagation, wave vectors necessarily change direction, eventually performing a complete rotation over a round trip. Moreover, (1) cannot describe more complex field distributions such as in Figs. 2b–d.

A more natural representation of the field on a sphere than plane waves [47], the spherical harmonics $Y_{lm}(\theta, \varphi)$ are the functions that subtend WGMs. In analogy with the quantum states of hydrogenoid atoms, l and m are referred to as the orbital and azimuthal numbers, respectively, of an electromagnetic mode. Among the Y_{lm}'s, those that correspond to intensity distribution as in Fig. 2 are such that $l, |m| \gg 1$, $l - |m| = O(1)$ [32, 48]. In that limit, all components of the electric field tend to be proportional to Y_{lm} [28, 32]. Hence, if (lm) and (LM) correspond to the fundamental and SH, respectively, the correct expression for the coupling constant is

$$\kappa = \iint \chi^{(2)} Y_{LM}^* Y_{lm}^2 \sin\theta \mathrm{d}\theta\mathrm{d}\varphi\,. \tag{11}$$

Above, $\chi^{(2)}$ is an appropriate combination of the components of the nonlinear susceptibility tensor, which depends on the precise vectorial structure of the electric field [28]. In the case where two fundamental modes $(l_1 m_1)$ and $(l_2 m_2)$ are excited and the sum-frequency is generated, (11) becomes

$$\kappa = \iint \chi^{(2)} Y_{LM}^* Y_{l_1 m_1} Y_{l_2 m_2} \sin\theta \mathrm{d}\theta\mathrm{d}\varphi\,. \tag{12}$$

Hence, if $\chi^{(2)}$ is uniform,

$$\kappa \propto \iint Y_{LM}^* Y_{l_1 m_1} Y_{l_2 m_2} \sin\theta \mathrm{d}\theta\mathrm{d}\varphi\,, \tag{13}$$

and it vanishes unless the quantum rules for angular momentum composition are satisfied [28, 29, 45, 49]:

$$M = m_1 + m_2\,, \qquad |l_1 - l_2| \leq L \leq l_1 + l_2\,. \tag{14}$$

In addition, conservation of parity with respect to the equator $\theta = \pi/2$ requires that $L + l_1 + l_2$ be even.

Aside from the angular dependence given by $Y_{lm}(\theta, \varphi)$, WGMs also have a specific radial dependence, given by $j_l(n\omega r/c)$ inside the sphere, where $j_l(x)$ is a spherical Bessel function [47], c is the speed of light in vacuum, and n is the index of refraction. The conditions of continuity of the tangent electric and magnetic fields at $r = a$ yield the characteristic equations for transverse electric (TE) and transverse magnetic (TM) modes. A number of theoretical works have been devoted to solving these characteristic equations in the large-l limit [50–53]. Especially useful is the formula derived in [50, 51]:

$$\omega_{l,p} \sim \frac{c}{na}\left[\nu + \alpha_p\left(\frac{\nu}{2}\right)^{1/3} - \frac{B}{(n^2-1)^{1/2}}\right], \tag{15}$$

where $\nu = l + 1/2$, α_p is the pth root of the Airy function $Ai(-z)$, and

$$B = \begin{cases} n & \text{for TE modes,} \\ 1/n & \text{for TM modes.} \end{cases}$$

The index p constitutes a third, 'radial', number for the sphere resonances, and effectively counts the number of maxima in the intensity distribution along the radial direction (see Fig. 2). Equation (15) can also be used for discs and toroidal cavities when $m = l$ [26, 46]. Once a set of

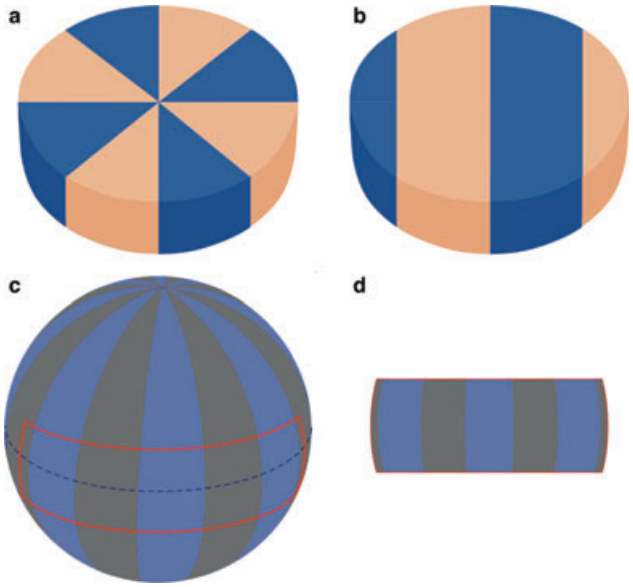

Figure 3 (online color at: www.lpr-journal.org) Quasi-phase matching patterns proposed for (a,b) a disc and (c,d) a spherical resonator [23, 28]. For technical convenience, the poling patterns (b) and (d) have been applied rather than (a) and (c) for the disc and sphere, respectively. Note in (c) that the coherence length is maximum at the equator and zero at the poles.

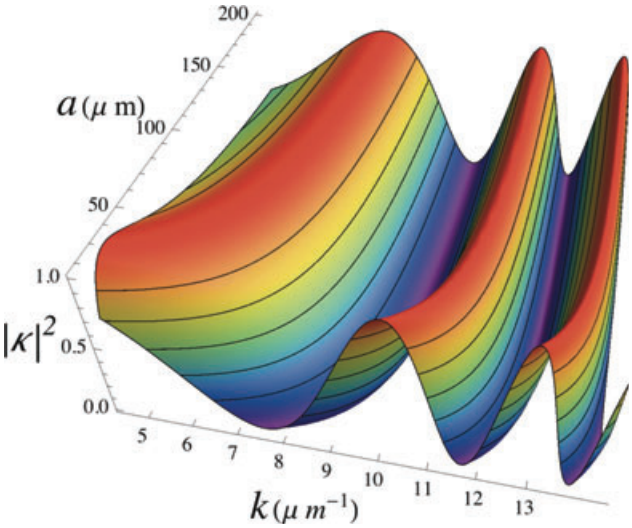

Figure 4 (online color at: www.lpr-journal.org) Coupling efficiency as a function of sphere radius a and fundamental vacuum wave number k from (17) for $\ell = 8.8\,\mu\mathrm{m}$.

WGMs are found that satisfy the phase matching conditions (14), one must ensure that the resonance condition

$$\omega_{L,P} = \omega_{l_1,p_1} + \omega_{l_2,p_2} \tag{16}$$

is also met. For isotropic spheres, this generally requires the radial number P of the SH to be larger than p_1 and p_2, to the detriment of good radial overlap between the modes [28, 29]. Such a difficulty was also reported with third harmonic generation [27].

Quasi-phase matching can be achieved through periodic modulation of the nonlinear susceptibility, as sketched in Fig. 3. To find the coherence length along the equator, let us restrict the integration in (11) to an angular sector of the sphere with arc length ℓ along the equator. For SHG with $l_1, l_2, m_1, m_2 = l$ and $M = L$, one easily finds

$$|\kappa|^2 \propto \sin^2\left(\frac{L-2l}{2a}\ell\right). \tag{17}$$

Hence, the coherence length along the equator is

$$\ell_c = \frac{\pi a}{L-2l}, \tag{18}$$

and along a parallel of polar angle θ, it is given by

$$\ell_c(\theta) = \frac{\pi a}{L-2l}\sin\theta. \tag{19}$$

In these expressions, both L and l are functions of the fundamental and SH frequencies through (15). Given a modulation half-period ℓ of the nonlinear susceptibility, optimal sphere size and optical frequency can be chosen by plotting (17), as in Fig. 4. With this method, fundamental radial numbers $P, p = 1$ can be selected, and optimal mode overlap can be achieved. As seen in Fig. 4, when the radius of the sphere changes, the locus of optimal conditions for SHG bends. This bending, which is more apparent when the sphere radius is small, is a consequence of the modal effective index dispersion. A periodic pattern based on this length would compensate both the material index dispersion and the modal effective index. Note from (19) that, away from the equator, the coherence length decreases, being maximum at the equator and zero at the poles. The periods of the optimal quasi-phase matching pattern thus resemble the curved surface of an orange slice, as shown schematically in Fig. 3. Recently, more complicated poling patterns were considered in relation to a toroidal cavity both theoretically [54] and experimentally [55] with the aim of a broader tunability.

Finally, in [24] and [41], it was recognized that the effective nonlinear susceptibility could vary along the azimuthal coordinate for an AlGaAs crystal. Indeed, the polarization of the electric field varies with the position along the equator, while the crystal axes do not. This modulates $\chi^{(2)}$ by a factor $\cos(2\varphi) = \cos(2s/a)$ in (12), which can be made to yield phase matching if the radius a is suitably chosen. More recently, the same approach was used for difference-frequency generation [56].

3. Experiments

3.1. Fabrication of nonlinear WGM resonators

To fabricate a nonlinear micro-resonator having a ring or spherical shape is not a straightforward task. Such a task is less demanding if third-order instead of second-order

nonlinearity is considered. In the former case a lack of inversion symmetry is not required and there are several examples where this has been achieved successfully [57]. One may use very isotropic material configurations such as micrometer-size liquid droplets [58]. However, to efficiently couple to WGMs it is more appropriate to use a solid-state-based technology. Visible third-harmonic generation has been achieved using toroidal micro-ring resonators [27]. Those rings were fabricated on oxidized silicon wafers in a four-step procedure that included photolithography performed to create disc-shaped photoresist pads, immersion in buffered HF solution at room temperature to etch a silica disc, exposure to XeF_2 gas for the purpose of isotropic selective removal of silicon and to obtain the silica disc on a pillar, and irradiation with a CO_2 laser to melt the periphery of the silica disc to turn the edges of the disc into a toroid [59]. If such wafer-based processing were to be applied to a non-centrosymmetric crystal, the stoichiometry and lack of inversion symmetry would most likely be lost in the last step where melting of the material is required. Ilchenko et al. proposed the fabrication of toroidal ring micro-resonators by diamond polishing of the rims of flat $LiNbO_3$ discs less than 1 mm thick. The mechanical polishing applied was such to allow one to reach quality factors as high as 2×10^8 [23, 26], and even higher quality factors were reported with more transparent materials, such as Al_2O_3 and CaF_2 [60]. With diamond polishing, surface roughness below 0.2 nm can now be obtained [61].

An alternative option for the fabrication of nonlinear circular micro-resonators is to combine melting-based fabrication for the resonator with subsequent deposition of a nonlinear material in such a way that non-centrosymmetry is preserved. It is possible to obtain a nearly perfect microsphere attached to a thin stem by melting the end of a commercial optical fiber [62]. The nonlinear material can then be deposited by simply dip-coating the surface of the sphere with a mono-molecular layer of nonlinear molecules. In the work reported in [63], an entire sphere together with its holding stem were immersed in a 1-propanol solution in which CV molecules were dissolved. Removing the stem and sphere from the solution at a constant speed of 1 mm/s produced a very homogeneous, one-molecule-thick, layer coating with a surface density that was proportional to the concentration of CV in the 1-propanol solution. This proportionality was confirmed by coating a set of flat substrates using the same technique with CV concentrations varying between 10^{-5} and 8×10^{-5} M. Measuring the absorption peak at 597 nm of these samples and using the estimated CV cross-section of $(11.5 \pm 0.3) \times 10^{-16}$ cm^2 at this wavelength, the number of molecules per unit surface could be determined. Fig. 5 illustrates the linear dependence of the surface concentration on the molarity of the dip-coating solution. This linear law can safely be extrapolated to concentrations below 10^{-4} M. This procedure offers a simple and effective way to tune the surface nonlinearity of nonlinear micro-resonators.

Finally, high-Q silicon [64] and AlGaAs [65] micro-disc resonators have been fabricated. These have the advantage of being suitable for telecommunications wavelengths and, in the case of AlGaAs, of displaying particularly large nonlinear coefficients. The cavities envisaged in [24, 41, 56] have a relatively small radius of 3.5 µm. This is necessary to achieve a sufficiently fast modulation of the effective nonlinear coefficient.

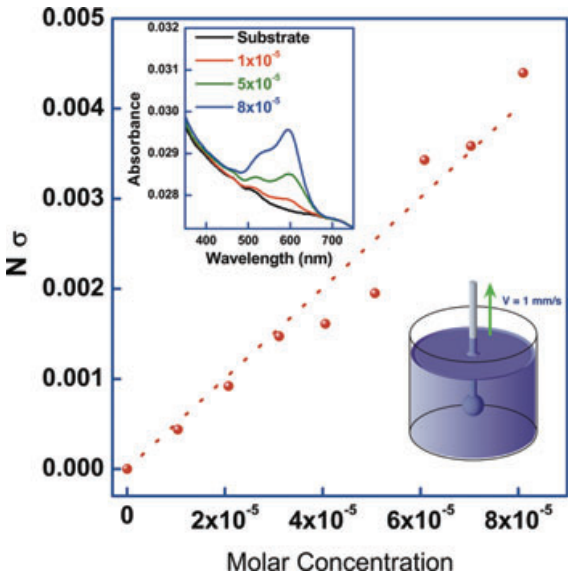

Figure 5 (online color at: www.lpr-journal.org) The number of CV molecules per unit surface times the cross-section of CV as a function of the molar concentration of the solution used for a coating layer. Inset: absorbance spectra for three monolayers representative of the eight monolayers prepared.

More details on the fabrication of WGM resonators can be found in [39].

3.2. Phase matching and quasi-phase matching of WGMs

For isotropic spheres, the frequency dispersion relation (15) of WGMs only allows phase matching between modes having different radial numbers [27–29]. On the other hand, for birefringent materials, type-I phase matching is possible, as was demonstrated by Fürst et al. with a $LiNbO_3$ disc resonator. They managed to achieve both (14) and (16) experimentally with $P, p_1, p_2 = 1$ for SHG [49] and optical parametric oscillation [66]. In their setup, the pump wave was a TM mode; it was thus polarized in the equatorial plane, with ordinary index of refraction. In contrast, the SH signal was a TE mode, polarized in the polar direction and subjected to extraordinary index of refraction. Because of the differential response of the two indices, phase matched WGMs could be brought into resonance by either applying a bias voltage to the cavity or controlling the temperature. Another approach was followed by Savchenkov et al., who tuned the frequency dispersion of WGMs through the thickness of a disc-shaped $LiNbO_3$ resonator [46]. With an appropriate thickness, a given set of phase matched modes could again be made resonant. On the other hand, with four-wave mixing, mediated by a third-order nonlinearity, it is possible

to parametrically generate a signal and idler waves with frequencies very close to those of the pump waves. The bulk index of refraction thus varies sufficiently little between the various frequencies that the frequency mismatch can be compensated by the Kerr effect [67, 68].

Quasi-phase matching consists of periodically distributing the nonlinear material. Such a periodic pattern must be composed of alternated domains, the arc length of which being exactly one coherence length of the corresponding nonlinear interaction. This coherence length is given for the case of spherical resonators in Eq. (19) as a function of the polar angle.

The first domain configuration to achieve quasi-phase matching in a disc-type cavity was proposed by Ilchenko et al. [23]. In the optimal configuration such a flat disc would have to be poled with domains distributed symmetrically with respect to the center of the disc, as shown in Fig. 3a. In other words, the arc length of each domain at a distance a from the center would be equivalent to $\pi a/\Delta m$, where Δm is the azimuthal number mismatch. A more practical, if less efficient, solution proposed in the same paper is to have poled stripes as in Fig. 3b. This can be obtained with commercially available periodically poled nonlinear crystals. With such a poling geometry, a WGM experiences a nonlinear grating with varying period. This configuration was implemented successfully to achieve parametric frequency doubling in a millimeter-size toroidal cavity made of periodically poled $LiNbO_3$ [26] (see Fig. 6). Later on, the poling technique was improved by maneuvering a micrometer-size electrode along the crystal surface, making it possible to inscribe almost any desired poling pattern in that material [69].

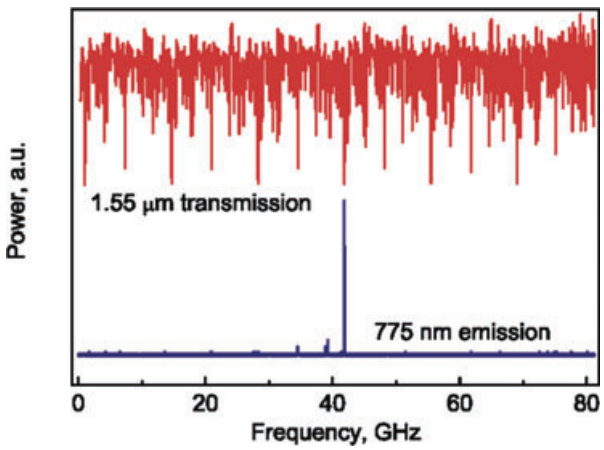

Figure 6 (online color at: www.lpr-journal.org) Fundamental transmission spectrum of a $LiNbO_3$ cavity (top) and SH emission spectrum (bottom). (Reprinted with permission from [26]. ©2004 American Physical Society.)

When the nonlinear material is only covering the surface of the resonator it is, in principle, possible to achieve a periodic grating with the correct pitch. Recently, it was shown that the nonlinearity of molecular layers deposited on a flat surface could be quenched at will using an electron beam gun [70]. Exploiting this effect, periodic $\chi^{(2)}$ patterns were inscribed on flat molecular films by means of a scanning electron microscope. From such gratings it was possible to measure SH diffraction patterns where the relative intensity of the diffraction orders observed agreed with the expectations for a sheet of nonlinear dipoles with a periodic modulation. However, no linear diffraction was seen, indicating that the procedure followed did not induce a periodic modulation in the real part of the refractive index. This technique was applied to obtain a nonlinear periodic grating on a portion of the surface of a microsphere [63]. The pattern inscribed was designed from the domain distribution that was determined from the phase matching condition obtained from an equation similar to Eq. (19). In general, patterning a non-flat surface would require xyz scanning in additional to rotational motion of the sphere. Indeed, to achieve a domain distribution covering the entire sphere, as the one shown in Fig. 3, would require a rotation of the sphere along the stem that holds it. In [63], the problem was circumvented by pattering only one-quarter of the sphere. This limited the conversion efficiency, but allowed one to demonstrate that the curved pattern designed yielded a SH peak at the spectral position predicted by the phase matching condition. The role played by phase matching for surface SHG in the WGMs was demonstrated by tuning the fundamental wavelength in a 100 nm spectral range. As shown in [63] and in Fig. 7, the SH signal peaks at the predicted wavelength of phase matching with a narrow bandwidth of just a few nanometers. The phase matching wavelength could be determined from Eq. (18) where the parameters used were the actual experimentally measured ones. As reported in [63], the sphere radius was accurately measured from a scanning

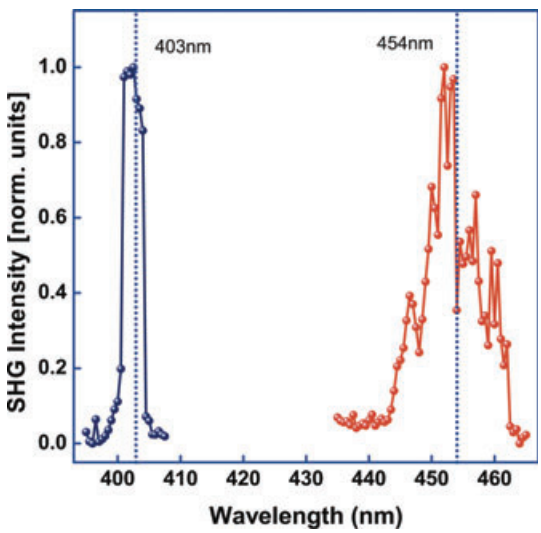

Figure 7 (online color at: www.lpr-journal.org) SHG as a function of half the wavelength of the fundamental wave when the pump wavelength is centered at 800 nm (blue spheres) and when centered at 900 nm (red spheres). The vertical dotted lines indicate the wavelength for the quasi-phase matching condition calculated using Eq. (18) and the experimentally measured values for the corresponding grating half-periods ℓ_c and sphere diameter. Lines between experimental points are guides for the eye.

electron microscopy image taken before writing the grating on the sphere. While in [63] the fundamental wavelength was close to 800 nm, we have used for the purpose of this review an optical parametric oscillator (OPO) to shift the fundamental wavelength to around 900 nm. In that case, the radius of the sphere was 124 µm and the grating pitch close to 10.2 µm. The phase matching peak obtained was broader than with the original laser-pumped sphere. This is due to the OPO output, which is broadened by 27 nm relative to the original laser pulse.

3.3. Pulse walk-off compensation

To reach measurable SH power levels when the nonlinear material is confined to an ultrathin surface layer or film, a pulsed generation is preferable to a continuous wave (CW) one. Indeed, while intensities of the order of 10^7 W/cm^2 can be reached inside a micro-resonator with a CW pump, peak values up to 10^{10} W/cm^2 can be attained with pulses. An additional advantage when using pulses stems from the broader bandwidth of them, which enables light coupling into several 'l' modes of the sphere, making phase matching more easily compatible with energy conservation. On the other hand, different group velocities for the fundamental and SH waves result in a temporal walk-off, meaning that the overlap of two 150 fs pulses is lost after a few tens of micrometers. Hence, with radii of approximately 180 µm, pulse overlap can be lost well before a single cavity round trip is completed. To circumvent this problem, the pump pulses should be stretched, to ensure permanent overlap as shown schematically in Fig. 8. This pulse stretching can be done with the same tapered fiber that is used to couple light into the WGMs of the circular micro-resonator. In the experiment in [63], 140 m of an optical fiber loop placed in between the entrance of the fiber and the tapered coupling region was found to yield optimal stretching. The resulting pulse length was close to 20 times the sphere perimeter. Given the interaction within a spherical cavity, overlap was preserved, no matter the distance traveled by the pulses.

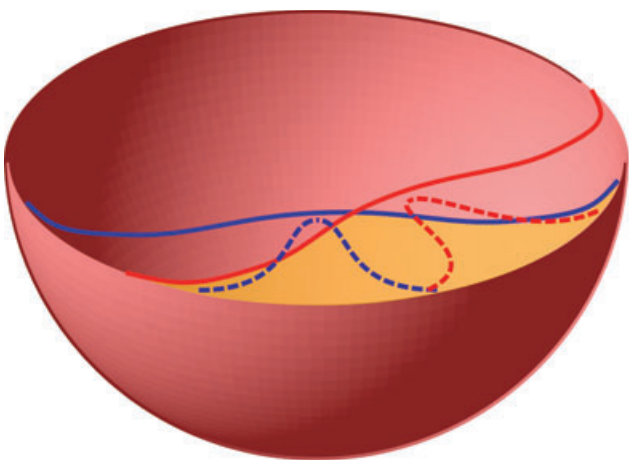

Figure 8 (online color at: www.lpr-journal.org) Schematic view of pulse walk-off in a microsphere when the pulses are coupled into the WGMs. The yellow area represents the region of overlap between the fundamental (red) and SH (blue) pulses when such pulses are stretched (solid lines) relative to the original pulses (dotted lines) which do not overlap.

3.4. Out-coupling the nonlinear generated light

Typically, pump laser light is coupled into a micro-resonator using either a prism coupler or, more often, a tapered optical fiber. In an up-conversion process, the tapered coupler is designed for efficient coupling of the infrared pump. Although this coupler is not phase matched in the visible region, typically it does allow enough coupling of the up-converted radiation back to the fiber for then to be measured at the exit tip of the fiber [27]. To make such a process more efficient, Carmon et al. recently developed a wide band (850 nm) fiber coupler to a whispering gallery cavity with ultrahigh quality factor [38]. It consisted of a bent-taper coupler whose design was intended to match closely toroidal whispering galleries. This, in turn, endowed the device with enhanced coupling bandwidth. The key idea of the proposed device was to provide a more symmetrical coupling geometry in which a tightly bent coupling mimicked the form factor (for dispersion) of the toroidal whispering gallery. Efficient input coupling to micro-toroid resonators over spans as large as 850 nm was demonstrated. This enhancement was achieved, in part, by compromising the output coupling efficiency and overall ideality, which was not as high as for the tapered fibers. Nonetheless, this compromise could result in acceptable output coupling efficiency over very broad wavelength spans. Alternative approaches may consider a dual-fiber coupling system where two taper couplers are placed tangentially at the opposite sides of the equator of a microsphere [8]. One serves as the input coupler and the other as the output coupler. This last approach, however, has not yet been implemented to out-couple light at double the frequency relative to the input light. It has also been suggested that thinning down the taper may prevent coupling of the up-converted light to a high-order transverse mode and consequently increase the coupling efficiency in the visible or UV generated light relative to the infrared pump. However, when using high peak power laser pulses, thinning down the taper may lead to an intense white light generation. Such white light would mix with the up-converted light which could no longer be filtered to be detected at the exit end of the coupling fiber. In that event, the Rayleigh scattered light from defects at the surface of the sphere could be collected, appropriately filtered, and detected separately from any other background light. Measuring up-conversion in WGMs from scattered light has been carried out successfully [27, 63].

3.5. SHG from a small number of molecules

The possibility to tailor the configuration of a nonlinear material separately from the specificities of a micro-resonator has allowed, very recently, the demonstration of SH light

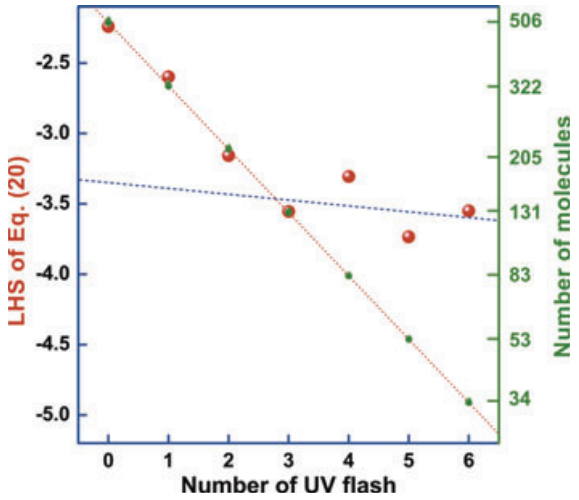

Figure 9 (online color at: www.lpr-journal.org) Sequence of 1 s UV flashes (horizontal axis). Left-hand side (LHS) of Eq. (20) where the variables correspond to the experimentally measured intensities (left vertical axis and red spheres). The background noise intensity is subtracted from the measured intensity and then this difference is divided by the reference input intensity to ensure a dimensionless logarithmic argument. The number of molecules on the surface is determined using Eq. (21), $N_0 = 506$, and α' is determined from the linear fit to the first four experimental data points (right vertical axis and green dots). Linear fit to the first four experimental data points (red dotted line). Linear fit to the last four experimental data points (blue dashed line).

generation from a very small number of molecules [63]. As we will discuss later in Sect. 4, this may have relevant implications for sensing devices meant to detect low concentrations of small molecules. The procedure used in [63] was to coat a microsphere resonator with low-concentration solutions of CV molecules and then inscribe a periodic grating following the electron beam technique described in Sect. 3.2. Such a nonlinear resonator was placed in the experimental setup where short light pulses from an amplified Ti:sapphire laser were coupled into the WGMs of the sphere. Then, a UV disinfection flashlamp was shone at 1 s intervals to degrade the CV molecules until the SH signal measured was down to noise level. In Fig. 9, the SH light intensity is shown as a function of the number of UV flashes. Given a background SH intensity noise $I_{\rm bg}$ and an initial number N_0 of active molecules, the measured SH intensity $I_{2\omega}$ is related to the fundamental pump intensity I_ω by [63]

$$\ln\sqrt{\frac{I_{2\omega}-I_{\rm bg}}{I_\omega}} = -\alpha' t + \ln\left(N_0\sqrt{\beta I_\omega}\right), \qquad (20)$$

where $I_{\rm bg}$ is the background signal noise at the SH frequency not coming from the molecules, $\alpha' = \alpha I_{\rm uv}$ (where $I_{\rm uv}$ is the UV intensity at the sphere surface), t is the illumination time, and α and β are constants of proportionality to ensure dimensional consistency. The slope of such a linear curve is directly linked to the rate at which the nonlinear activity of the molecules is destroyed by the UV lamp. Indeed, the number of molecules that remain active on the surface can easily be shown to evolve as

$$N = N_0 {\rm e}^{-\alpha' t}. \qquad (21)$$

As described in Sect. 3.1, the surface density of CV molecules can be deduced from the molarity of the coating solution. Provided that the interaction surface region is limited to the portion of the sphere surface where the periodic grating simultaneously overlaps with the two interacting waves, the initial number of molecules participating in SHG is calculated to be 506±9. In the last UV flash before the signal goes down to noise level, 75 molecules are destroyed. As shown in Fig. 9, the signal-to-noise ratio amounts to a dispersion in the number of molecules close to 50, implying that approximately 50 to 100 molecules are needed to measure a change in the SH light. This result confirms the relevant role played by such high-Q microspheres. By comparison, when molecules are deposited on a flat transparent substrate, using laser pulses with a peak intensity very close to the damage threshold of the substrate or molecules, one would typically need 10^{10} molecules to obtain a measurable signal.

4. Conclusion and outlook

The study of nonlinear optical processes, especially those of second order, in spherical geometry has led to the re-examination of the question of phase matching. This is particularly relevant for large circular geometries forming WGM resonators. It was gradually realized that the usual rule of linear momentum conservation gives way to angular momentum conservation, with the same selection rules as those found in quantum mechanics.

Very recently, two new significant steps towards the control of the nonlinear interaction in ring or spherical resonators were made. The former led to the enhancement of the nonlinear interaction in the bulk of the resonator [49,66], and the latter achieved quasi-phase matched nonlinear surface interaction [63]. Based on these results, several interesting advances are in view. On the one hand, perfectly phase matched nonlinear interaction can be used to design highly efficient OPOs. On the other hand, WGMs can be used to nonlinearly sense the presence of small quantities of a given substance which may be deposited on the surface of the resonator.

The recent demonstration of low-threshold parametric oscillation opened the door to the development of compact, stable, low-power tunable spectroscopy sources with narrow linewidth. The high Q of the WGM interaction in such sources may find useful applications in quantum optics where a large ratio for the nonlinear interaction when compared to losses or other sources of noise is essential. Parametric down-conversion using sub-threshold parametric oscillators and parametric amplifiers has been a very successful strategy for the generation of quantum optical states such as squeezed light [71, 72], entangled photon pairs [73], and heralded single photons [74]. It is natural to ask what advantages nonlinear micro-resonators may offer

for these applications in quantum optics. While quantum state generation is beyond the scope of this review, we make some general observations. Parametric down-conversion is almost always performed in a low-gain regime, often with optimum gain found between a tenth and a half of the threshold for oscillation. As such, low-threshold oscillators may enable the realization of quantum optical sources with extremely low pump powers [66, 75]. At the same time, the degree of squeezing is often limited by losses, either within the resonator or on collection/out-coupling. High Q and large coupling efficiencies of micro-resonators are thus especially attractive for squeezing applications, while low-loss coupling into fibers may make practical the distribution of highly squeezed states over large distances. Experiments with entangled pairs can also benefit from low thresholds. While these photon counting experiments are far less sensitive to losses, they are highly sensitive to background from other processes [76]. For this reason, the practical application to quantum light generation may depend on features of the resonator and nonlinear material not directly related to the nonlinear process itself. A survey of the many difficulties encountered in generating squeezed states is given in [77]. Aside from quantum optics, Fürst et al. [66] suggested other areas of physics where low-threshold WGM OPOs might find applications, such as to investigate the rich dynamic phenomena in the far-above-threshold regime or to combine the optical nonlinearity with optomechanics.

The quasi-phase matched SHG in WGMs from molecules on the surface of a sphere may prove to be very effective as a sensing mechanism. A versatile sensing device must be capable of detecting label-free or unmarked objects, exhibit a high sensitivity, and be able to distinguish positive signals coming from the object to be detected from signals triggered by other unwanted objects present in the environment of the device. Label-free detection can be achieved when the property on which the sensing device is based is shared by many different types of objects. As indicated in the introduction, generation of light via a quadratic nonlinear process is rather universal since all forms of matter may be used, in principle, to generate a SH. SHG has already been applied successfully for label-free multichannel biosensing [78] and also to detect the signal from very small nitrate molecules at an interface [79]; such molecules are difficult to visualize with other optical systems.

To reach large sensitivities, in some optical devices one may take advantage of an optical cavity configuration that would allow for the light to interact elastically many times with the object to be detected. The number of interactions is simply given by the ratio of the photon cavity lifetime to the round-trip time, which can be computed as

$$\frac{Q\Delta\nu_{\mathrm{fsr}}}{2\pi\nu},$$

where $\Delta\nu_{\mathrm{fsr}}$ is the free-spectral range and ν is the frequency (in Hz). This is, essentially, the cavity finesse. Such a number becomes close to one million when microsphere resonators with Q factors of 10^8–10^9 are used. The pioneering use of WGMs in microspheres for sensing considered the detection of proteins adsorbed on the surface of the spheres. The resulting increase of the resonator volume leads to a larger optical path along the equator, and hence to a detectable red-shift of the WGM resonances [80–82]. It has been noted that the power dissipated by a molecule could also result in a resonance shift through the thermal dependence of the refractive index in the sphere. This thermo-optic effect is distinct from the reactive effect described in [80], which is power-independent. However, attempts to increase the sensitivity with the thermo-optic effect have produced no reliable results, and a recent theoretical comparison between the two mechanisms, thermo-optics and reactive, concluded that no significant enhancement could be obtained from the thermo-optic effect [83]. Measuring the resonance shift was also applied to detect other types of single objects, such as the influenza A virus [84] and nanospheres [85]. As for the detection of single objects, at the time of writing, maximum sensitivity can be achieved when a thermally stabilized reference interferometer is used in conjunction with a WGM microcavity [86].

For all such configurations to be effective in a detection device for a given small object, there must be a mechanism or design capable of distinguishing the object to be detected from another one that, if bound to the sensing area of the device, would produce a similar signal to that of the object to be detected. Binding sites selective to the object to be detected are typically used to prevent unwanted molecules or objects from attaching themselves to the surface of ring or spherical micro-resonators.

As discussed above, any object attached to an interface can be used for SHG enhancement owing to the lack of inversion symmetry of the interface. Labeling of the object with, for instance, a fluorescent chromophore is not required. To enhance the effectiveness of light generation, it is not a condition for the molecules to be large. For instance, an acceptor-donor character would also enhance the nonlinear interaction. For the sake of comparison, 100 of the molecules used in [63] and in Sect. 3.5 occupy a volume that is approximately three orders of magnitude smaller than the nanoparticles used in [86]. At the moment, in terms of concentration, resonance shift-based systems present a clear advantage, while SHG-based ones are more suitable for the detection of extremely small objects.

The quasi-phase matching mechanism required to obtain effective SHG provides in itself the means to avoid the detection of unwanted objects. To sense a specific type of molecule by SHG using microsphere resonators, one would have to cover them with a monolayer surface of molecular sites where the specific molecule to be detected would bind. To obtain enhanced quasi-phase matched SHG, one would have to previously periodically pattern such a monolayer of sites, as shown schematically in Fig. 10. This could be performed using electron beam periodic patterning [87] similar to that implemented in [63]. In such a way, molecules would bind more effectively to the proper stripes on the sphere surface and quasi-phase matching would be possible. Note that, even in the case where single-molecule detection is considered, the same periodic patterning is necessary. Otherwise, if the molecules were to be adsorbed anywhere on the surface, the contribution from a given molecule would

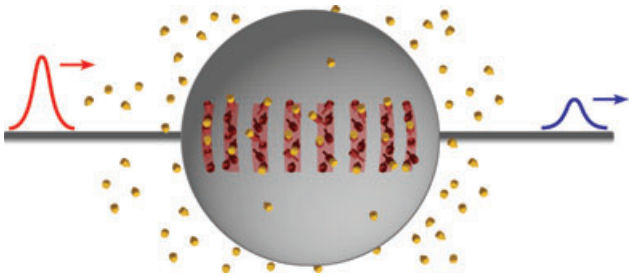

Figure 10 (online color at: www.lpr-journal.org) Schematic representation of a microsphere prepared for sensing suspended molecules (orange). The sites (red) where the molecules bind are periodically patterned to achieve phase matched SHG. The SH signal coupled out of the resonator would increase progressively as molecules bind to the sites.

be cancelled by the contribution from another molecule separated a distance equivalent to twice the coherence length. When the surface is patterned, if unwanted highly nonlinear molecules are adsorbed anywhere on the surface, the SHG from these molecules would remain down to noise level as was demonstrated in [63]. Note that, except for very specific radii and conditions, the contribution from the resonator surface would not be phase matched. Such a contribution could not grow even if the value of Q were high.

There are, still, many issues to be resolved before SHG in WGMs can be effectively used in very sensitive sensing. For instance, work must be done on reducing the area aspect ratio between the sensitive part of the sphere surface and the one that does not contribute to sensing. A possible path to markedly reduce the molecular concentration needed for detection might be by forming arrays of spheres, which would be coupled to each other in order to enhance the sensitivity to concentration, forming what could be named an optical nose. We see, however, that the work performed over the last fifteen years in the field of SHG in circular geometries and WGMs in ring or spherical micro-resonators has laid the foundations for the development of such new types of sensing devices with unsurpassed detection sensitivity.

Finally, as commented above, the interest in nonlinear optics in ring or spherical micro-resonators is not limited to sensing. Fundamental aspects of physics, such as quantum state entanglement or cavity-enhanced nonlinear interactions, are still to be found in such circular geometries.

Acknowledgements. We thank Morgan Mitchell for helpful discussions on quantum applications. We acknowledge the Ministerio de Ciencia e Innovación which supported the work under grants MAT2008-00910/NAN and CONSOLIDER NANOLIGHT CSD2007-00046. G. K. is a Research Associate with the Fonds de la Recherche Scientifique (FRS-FNRS, Belgium). J. L. D.-J. was supported by a México CONACYT grant (grant no. 187592).

Received: 12 April 2011, **Revised:** 19 May 2011, **Accepted:** 19 May 2011

Published online: 4 July 2011

Key words: Whispering gallery modes, second harmonic generation, micro-resonators, nonlinear scattering.

Gregory Kozyreff obtained his Ph. D. at the Université libre de Bruxelles in 2001 with a thesis on nonlinear laser dynamics. From 2001 to 2004, he was as a post-doc at the Oxford Centre for Industrial and Applied Mathematics (OCIAM). In 2006, he visited ICFO-The Institute of Photonics Sciences. He is now a Research Associate of the F. R. S.-FNRS (Belgium). His current research activities include the study of nonlinear waves and patterns in spatially extended system, optics in micro-spheres, and the mathematical modeling of photovoltaic devices.

Jorge Luis Dominguez received the Bachelor degree in telecommunications engineering from Autonoma National University of Mexico (UNAM) in 2003 and his Master Degree from the University Polytechnic of Catalunya (UPC), Spain in 2006. He has previously held position in a telecommunications company (Avantel) and is currently finishing his Ph. D. degree at the Institute of Photonics Sciences (ICFO) in Jordi Martorell's group. In 2010 he held a position as a specialist manufacturer of advanced solid-state instruments for laser tuning (Radiantis). His research interests are in optical nonlinear frequency mixing, photonic integrated circuits, electron-beam lithography, non-linear optical systems, all-semiconductor integrated parametric devices, circular microresonators, nanowires and nanofabrication.

Jordi Martorell obtained a Ph. D. in physics from Brown University, in 1990. Since then his research focused to study light-matter interactions in photonic nanostructured materials. Later, he became a Professor at the Universitat Politècnica de Catalunya where he laid the groundwork for the study of the nonlinear interaction within ordered nano-structures. In 2005, he joined ICFO-The Institute of Photonics Sciences where he extended the study of the nonlinear interaction to materials that exhibit a random distribution of the nonlinear domains and to spherical high Q micro-resonator cavities. More recently, he has focused the core of his research to study the optical control provided by photonic nano-structures to enhance the performance of photovoltaic cells.

References

[1] M. M. Fejer, G. A. Magel, H. Jundt, and R. L. Byer, IEEE J. Quantum Electron. **28**, 2631 (1992).
[2] J. Martorell, R. Vilaseca, and R. Corbalán, Scattering of second harmonic light from small spherical particles, in: Quantum Electronics and Laser Science Conference, (Washington DC, USA, 1995), p. 32.
[3] J. Martorell, R. Vilaseca, R. Corbalán, and J. Trull, Second harmonic scattering from sites of a crystalline lattice, in: Pho-

tonic Band Gap Materials, edited by C. Soukoulis (Kluwer Academic Publishers, 1996), pp. 529–534.
[4] J. Martorell, R. Vilaseca, and R. Corbalán, Phys. Rev. A **55**, 4520 (1997).
[5] J. Martorell, R. Vilaseca, and R. Corbalán, Appl. Phys. Lett. **70**, 702 (1997).
[6] H. Wang, E. C. Y. Yan, E. Borguet, and K. B. Eisenthal, Chem. Phys. Lett. **259**, 15 (1996).
[7] N. Yang, W. E. Angerer, and A. G. Yodh, Phys. Rev. Lett. **87**, 103902 (2001).
[8] J. I. Dadap, J. Shan, K. B. Eisenthal, and T. F. Heinz, Phys. Rev. Lett. **83**, 4045–4048 (1999).
[9] V. L. Brudny, B. S. Mendoza, and W. L. Mochán, Phys. Rev. B **62**, 11152 (2000).
[10] J. I. Dadap, J. Shan, and T. F. Heinz, J. Opt. Soc. Am. B **21**, 1328–1345 (2004).
[11] Y. Pavlyukh and W. Hübner, Phys. Rev. B **70**, 245434 (2004).
[12] C. I. Valencia, E. R. Méndez, and B. S. Mendoza, J. Opt. Soc. Am. B **20**, 2150–2161 (2003).
[13] C. I. Valencia, E. R. Méndez, and B. S. Mendoza, J. Opt. Soc. Am. B **21**, 36–44 (2004).
[14] J. I. Dadap, Phys. Rev. B **78**, 205322 (2008).
[15] S. Roke, M. Bonn, and A. V. Petukhov, Phys. Rev. B **70**, 115106 (2004).
[16] S. Viarbitskaya, V. Kapshai, P. van der Meulen, and T. Hansson, Phys. Rev. A **81**, 053850 (2010).
[17] A. A. Fedyanin, O. A. Aktsipetrov, D. A. Kurdyukov, V. G. Golubev, and M. Inoue, Appl. Phys. Lett. **87**, 151111 (2005).
[18] P. P. Markowicz, H. Tiryaki, H. Pudavar, P. N. Prasad, N. N. Lepeshkin, and R. W. Boyd, Phys. Rev. Lett. **92**, 083903 (2004).
[19] A. Molinos-Gómez, M. Maymó, X. Vidal, D. Velasco, J. Martorell, and F. López-Calahorra, Adv. Mater. **19**, 3814 (2007).
[20] Y. Maruyama, M. Ishikawa, and H. Satozono, J. Am. Chem. Soc. **118**, 6257 (1996).
[21] M. Maymó, J. Martorell, A. Molinos-Gómez, and F. López-Calahorra, Opt. Exp. **14**, 2864–2872 (2006).
[22] X. Vidal, J. R. Herance, J. Marquet, J. L. Bourdelande, and J. Martorell, Appl. Phys. Lett. **91**, 081116 (2007).
[23] V. S. Ilchenko, A. B. Matsko, A. A. Savchenkov, and L. Maleki, J. Opt. Soc. Am. B **20**, 1304–1308 (2003).
[24] Y. Dumeige and P. Féron, Phys. Rev. A **74**, 063804 (2006).
[25] Y. Dumeige and P. Féron, Phys. Rev. A **76**, 035803 (2007).
[26] V. S. Ilchenko, A. A. Savchenkov, A. B. Matsko, and L. Maleki, Phys. Rev. Lett. **92**, 043903 (2004).
[27] T. Carmon and K. J. Vahala, Nature Phys. **3**, 430–435 (2007).
[28] G. Kozyreff, J. L. Dominguez Juarez, and J. Martorell, Phys. Rev. A **77**, 043817 (2008).
[29] Y. Xu, M. Han, A. Wang, Z. Liu, and J. R. Heflin, Phys. Rev. Lett. **100**, 163905 (2008).
[30] A. Serpengüzel, S. Arnold, and G. Griffel, Opt. Lett. **20**, 654–656 (1995).
[31] J. C. Knight, G. Cheung, F. Jacques, and T. A. Birks, Opt. Lett. **22**, 1129–1131 (1997).
[32] B. E. Little, J. P. Laine, and H. Haus, J. Lightwave Technol. **17**, 704 (1999).
[33] M. L. Gorodetsky and V. S. Ilchenko, J. Opt. Soc. Am. B **16**, 147–154 (1999).
[34] M. Cai, O. Painter, and K. J. Vahala, Phys. Rev. Lett. **85**, 74–77 (2000).
[35] A. Morand, K. Phan-Huy, Y. Desieres, and P. Benech, J. Lightwave Technol. **22**, 827–832 (2004).
[36] I. D. Chremmos and N. K. Uzunoglu, J. Opt. Soc. Am. A **23**, 461–467 (2006).
[37] H. Konishi, H. Fujiwara, S. Takeuchi, and K. Sasaki, Appl. Phys. Lett. **89**, 121107 (2006).
[38] T. Carmon, S. Y. T. Wang, P. Ostby, and K. J. Vahala, Opt. Exp. **15**, 7677–7681 (2007).
[39] A. B. Matsko and V. S. Ilchenko, IEEE J. Sel. Topics Quantum Electon. **12**, 3–14 (2006).
[40] V. S. Ilchenko and A. B. Matsko, IEEE J. Sel. Topics Quantum Electon. **12**, 15–32 (2006).
[41] Z. Yang, P. Chak, A. D. Bristow, H. M. van Driel, R. Iyer, J. S. Aitchison, A. I. Smirl, and J. E. Sipe, Opt. Lett. **32**, 826–828 (2007).
[42] R. W. Boyd, Nonlinear Optics (Academic Press, Inc., 1992).
[43] Z. Y. Ou and H. J. Kimble, Opt. Lett **18**, 1053 (1993).
[44] D. Braunstein, A. M. Khazanov, G. A. Koganov, and R. Shuker, Phys. Rev. A **53**, 3565–3572 (1996).
[45] M. V. Jouravlev and G. Kurizki, Phys. Rev. A **70**, 053804 (2004).
[46] A. A. Savchenkov, A. B. Matsko, M. Mohageg, D. V. Strekalov, and L. Maleki, Opt. Lett. **32**, 157–159 (2007).
[47] J. D. Jackson, Classical Electrodynamics, 3 edition (Wiley, 1999).
[48] L. W. Casperson, J. Opt. Soc. A. **65**, 399–403 (1975).
[49] J. U. Fürst, D. V. Strekalov, D. Elser, M. Lassen, U. L. Andersen, C. Marquardt, and G. Leuchs, Phys. Rev. Lett. **104**, 153901 (2010).
[50] S. Schiller and R. L. Byer, Opt. Lett. **16**, 1138–1140 (1991).
[51] C. C. Lam, P. T. Leung, and K. Young, J. Opt. Soc. Am. B **9**, 1585 (1992).
[52] S. Schiller, Appl. Opt. **32**, 2181–2185 (1993).
[53] I. H. Agha, J. E. Sharping, M. A. Foster, and A. L. Gaeta, Appl. Phys. B **83**, 303–309 (2006).
[54] D. Haertle, Journal of Optics **12**, 035202 (2010).
[55] T. Beckmann, H. Linnenbank, H. Steigerwald, B. Sturman, D. Haertle, K. Buse, and I. Breunig, Phys. Rev. Lett. **106**, 143903 (2011).
[56] A. Andronico, X. Caillet, I. Favero, S. Ducci, V. Berger, and G. Leo, J. Europ. Opt. Soc. Rap. Public. **3**, 08030 (2008).
[57] F. Treussart, V. S. Ilchenko, J. F. Roch, J. Hare, V. Lefèvre-Seguin, J. M. Raimond, and S. Haroche, Eur. Phys. J. D **1**, 235–238 (1998).
[58] D. H. Leach, W. P. Acker, and R. K. Chang, Opt. Lett. **15**(16), 894–896 (1990).
[59] D. K. Armani, T. J. Kippenberg, S. M. Spillane, and K. J. Vahala, Nature **421**(6926), 925–928 (2003).
[60] A. A. Savchenkov, V. S. Ilchenko, A. B. Matsko, and L. Maleki, Phys. Rev. A **70**, 051804(R) (2004).
[61] I. S. Grudinin, A. B. Matsko, A. A. Savchenkov, D. Strekalov, V. S. Ilchenko, and L. Maleki, Opt. Commun. **265**, 33 (2006).
[62] M. L. Gorodetsky, A. Savchenkov, and V. S. Ilchenko, Opt. Lett. **21**, 453–455 (1996).
[63] J. L. Dominguez-Juarez, G. Kozyreff, and J. Martorell, Nat. Commun. **2**, 254 (2011).
[64] M. Borselli, T. Johnson, and O. Painter, Opt. Express **13**(5), 1515–1530 (2005).
[65] K. Srinivasan, M. Borselli, T. J. Johnson, P. E. Barclay, O. Painter, A. Stintz, and S. Krishna, Appl. Phys. Lett. **86**, 151106 (2005).
[66] J. U. Fürst, D. V. Strekalov, D. Elser, A. Aiello, U. L. Andersen, C. Marquardt, and G. Leuchs, Phys. Rev. Lett. **105**, 263904 (2010).

[67] T. J. Kippenberg, S. M. Spillane, and K. J. Vahala, Phys. Rev. Lett. **93**, 083904 (2004).
[68] A. A. Savchenkov, A. B. Matsko, D. Strekalov, M. Mohageg, V. S. Ilchenko, and L. Maleki, Phys. Rev. Lett. **93**, 243905 (2004).
[69] M. Mohageg, D. Strekalov, A. Savchenkov, A. Matsko, V. Ilchenko, and L. Maleki, Opt. Express **13**(9), 3408–3419 (2005).
[70] J. L. Dominguez-Juarez, R. Macovez, M. U. Gonzalez, and J. Martorell, Appl. Phys. Lett. **97**, 023307 (2010).
[71] L. A. Wu, H. J. Kimble, J. L. Hall, and H. Wu, Phys. Rev. Lett. **57**, 2520 (1986).
[72] H. Vahlbruch, M. Mehmet, S. Chelkowski, B. Hage, A. Franzen, N. Lastzka, S. Goßler, K. Danzmann, and R. Schnabel, Phys. Rev. Lett. **100**, 033602 (2008).
[73] Z. Ou and Y. Lu, Phys. Rev. Lett. **83**, 2556 (1999).
[74] F. Wolfgramm, Y. A. de Icaza Astiz, F. A. Beduini, A. Cere, and M. W. Mitchell, Phys. Rev. Lett. **106**, 053602 (2011).
[75] J. U. Fürst, D. V. Strekalov, D. Elser, A. Aiello, U. L. Andersen, C. Marquardt, and G. Leuchs, Phys. Rev. Lett. **106**, 113901 (2011).
[76] X. Li, C. Liang, K. Fook Lee, J. Chen, P. L. Voss, and P. Kumar, Phys. Rev. A **73**, 052301 (2006).
[77] H. J. Kimble, Physics Reports **219**, 227 (1992).
[78] K. Tsuboi, S. Fukuba, R. Naraoka, K. Fujita, and K. Kajikawa, Appl. Opt. **46**, 4486 (2007).
[79] D. E. Otten, P. B. Petersen, and R. J. Saykally, Chem. Phys. Lett. **449**, 261 (2007).
[80] F. Vollmer, D. Braun, A. Libchaber, M. Khoshsima, I. Teraoka, and S. Arnold, Applied Physics Letters **80**, 4057–4059 (2002).
[81] S. Arnold, M. Khoshsima, I. Teraoka, S. Holler, and F. Vollmer, Opt. Lett. **28**, 272–274 (2003).
[82] F. Vollmer and S. Arnold, Nat Methods **5**, 591–596 (2008).
[83] S. Arnold, S. I. Shopova, and S. Holler, Opt. Express **18**, 281 (2010).
[84] F. Vollmer, S. Arnold, and D. Keng, Proc. Natl. Acad. Sci. USA **105**, 20701 (2008).
[85] J. Zhu, S. Ozdemir, Y. Xiao, L. Li, L. He, D. Chen, and L. Yang, Nature photonics **4**, 46–49 (2009).
[86] T. Lu, H. Lee, T. Chen, S. Herchak, J. Kim, S. Fraser, R. Flagan, and K. Vahala, Proc. Natl. Acad. Sci. USA **108**, 5976 (2011).
[87] C. K. Harnett, K. M. Satyalakshmi, and H. G. Craighead, Appl. Phys. Lett. **76**, 2466 (2000).